

**INVESTIGATION OF DIFFERENT TARGET-  
PROJECTILE COMBINATIONS FOR THE  
SYNTHESIS OF Z=120 ELEMENT**

*A Thesis submitted in partial fulfillment of the requirements for the award of  
degree of*

**Master of Science**

**In**

**Physics`**

**SUBMITTED BY**

MEHAK SHARMA

Roll No. 301504021

**UNDER THE SUPERVISION OF**

Dr. RAJ KUMAR

Assistant Professor of Physics

SPMS

Thapar University, Patiala



School of Physics and Materials Science (SPMS),

Thapar University,

Patiala-147004, India

July, 2017

*Dédié à mes parents et  
amis*

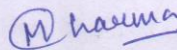
*(Dedicated to my parents and friends)*

## CERTIFICATE

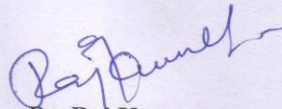
I hereby certify that the work which has been presented in this thesis entitled **“INVESTIGATION OF DIFFERENT TARGET-PROJECTILE COMBINATIONS FOR THE SYNTHESIS OF Z=120 ELEMENT”** submitted in partial fulfillment of the requirements for the award of degree of **Master of Science in Physics at Thapar University, Patiala**, is an authentic record of my own work carried out under the supervision of **Dr. Raj Kumar, Assistant Professor, SPMS** and refers other researcher's work which are duly listed in reference section.

The matter embodied in this thesis has not been submitted for the award of any other degree of this or any other university.

Date: 14/7/17

  
Mehak Sharma

This is to certify that the above statement made by the candidate is correct and true to best of my knowledge.

  
**Dr. Raj Kumar**

Assistant Professor,

School of Physics and Materials Sciences (SPMS),

Thapar University, Patiala

## ACKNOWLEDGEMENT

The writing and completion of this Dissertation wouldn't have been possible without the assistance, support and guidance of following of a few very special people in my life. First of all, I want to show my gratitude towards my creator for giving me strength and capability to complete this work.

I am really fortunate that, I had the kind association as well as supervision of **Dr. Raj Kumar**, Assistant Professor, School of Physics and Materials Science, Thapar University, Patiala. I cannot express my enough thanks to my supervisor for their continued encouragement and support.

My completion of this work couldn't have been accomplished without the support of my mentor **Miss Ishita Sharma**, such an intelligent and humble person, who has really given me all her support. Thanks a lot!

A special thanks to my classmates, friends and buddies especially Vrinda, Shivangi and Harjeet Singh for their countless times help throughout my journey in college. May god bless you all and have happier lives.

To my family, I won't be this stronger without you as my inspiration. You are the reason why I keep pushing; I keep facing all the struggles, pains and hardships. I love you so much!

Patiala

July, 2017

Mehak Sharma

## **ABSTRACT**

After, the latest addition to the periodic table the heaviest i.e.  $Z=118$ , Oganesson (Og) which was formally named on 28 November 2016, a rush has been started in the search of next stable island and towards the synthesis of superheavy element  $Z=120$ . Many experimental and theoretical approaches are being performed in hot and cold fusion approaches, in order to have better understanding regarding the stability of the completely fused compound nuclear system. For the elements  $Z>113$ , hot fusion approach is mostly preferred as they demand more asymmetric combinations and hence sustain fusion cross-sections, which are here calculated using the Wong formula for the four most suitable combinations, predicted till now. The fusion cross-sections of chosen reactions are calculated with quadrupole ( $\beta_2$ ) deformations and hot-optimized orientations. Also, using fragmentation potentials, we have tried to find some new combinations for  $^{302}120$ .

The following composition contains 3 chapters.

**CHAPTER 1:** gives an abstract of the nuclear fusion reaction dynamics in superheavy region and the different approaches that have been used till now in the process of synthesization. A brief discussion about the different types of deformations and orientations is stated along with their effects on the fusion dynamics. Also on the basis of some predictions regarding the synthesis of  $Z=120$ , for our present work we prefer to use the following projectile-target combinations i.e.  $^{54}\text{Cr} + ^{248}\text{Cm}$ ,  $^{50}\text{Ti} + ^{249}\text{Cf}$ ,  $^{50}\text{Ti} + ^{252}\text{Cf}$ ,  $^{48}\text{Ca} + ^{254}\text{Fm}$ .

**CHAPTER 2:** describes the total fusion cross-section as a product of capture cross-section calculated using Wong formula for deformed and oriented nuclei and probability of formation of compound nucleus  $P_{\text{CN}}$ . Also, the fragmentation potential and various interactions potential such as Coulomb potential, proximity potential and centrifugal potential are described.

**CHAPTER 3:** contains Wong formula based calculations for the above mentioned reactions and the fragmentation potentials are inspected for  $^{302}120$ .

# LIST OF FIGURES

## CHAPTER 1

**Fig.1.1** Formation of a heavier nucleus via neutron capture followed by  $\beta$ -decay and  $\gamma$ -rays emission.

**Fig.1.2** Island of Stability showing stabilities in super heavy region.

**Fig.1.3** Potential Barrier v/s the separation distance between the nuclei.

**Fig.1.4** Nuclear charge distribution in (a) spherical and (b) deformed case.

**Fig.1.5** Quadrupole deformed shapes of a nucleus (a) Oblate and (b) Prolate.

**Fig.1.6** Systematic diagram of quadrupolar nuclei with optimized orientations for “cold-elongated” configurations.

**Fig.1.7** Systematic diagram of quadrupolar nuclei with optimized orientations for “hot-compact” configurations.

## CHAPTER 3

**Fig.3.1** Scattering potential v/s separation distance R (fm) for four different entrance channels (a)  $^{50}\text{Ti} + ^{252}\text{Cf}$ , (b)  $^{50}\text{Ti} + ^{249}\text{Cf}$ , (c)  $^{54}\text{Cr} + ^{248}\text{Cm}$  and (d)  $^{48}\text{Ca} + ^{254}\text{Fm}$ .

**Fig.3.2** Fragmentation potential v/s mass fragment  $A_2$  for  $^{302}120$  at  $\ell = 0\hbar$ ,  $T=0$  MeV and  $\Delta R = 1.5$  fm.

**Fig.3.3** Fragmentation potential v/s mass fragment  $A_2$  for  $^{302}120$  at  $\ell = 0\hbar$ ,  $T=1$  MeV and  $\Delta R = 1.5$  fm for the decay of  $^{302}120$  nuclei.

**Fig.3.4** Fragmentation potential v/s mass fragment  $A_2$   $^{302}120$  at  $\ell = \ell_{\max}$ ,  $T=1$  MeV and  $\Delta R = 1.5$  fm for the decay of  $^{302}120$  nuclei.

**Fig.3.5** Scattering potential v/s separation distance R (fm) for the obtained reactions from minima's in fragmentation plot. (See Fig.3.3 and 3.4)

# LIST OF TABLES

## CHAPTER 1

**Table 1.1** Elements synthesized via Cold fusion.

**Table 1.2** Elements synthesized via hot fusion.

## CHAPTER 3

**Table 3.1** Comparison of the fusion probabilities at the potential barrier for the hot- fusion combinations  $^{50}\text{Ti} + ^{252}\text{Cf}$ ,  $^{50}\text{Ti} + ^{249}\text{Cf}$ ,  $^{54}\text{Cr} + ^{248}\text{Cm}$  and  $^{48}\text{Ca} + ^{254}\text{Fm}$ .

**Table 3.2** The calculated values of fusion cross-sections and  $P_{\text{CN}}$  for  $^{54}\text{Cr} + ^{248}\text{Cm}$ .

**Table 3.3** The calculated values of fusion cross-sections and  $P_{\text{CN}}$  for  $^{50}\text{Ti} + ^{249}\text{Cf}$ .

**Table 3.4** The calculated values of fusion cross-sections and  $P_{\text{CN}}$  for  $^{50}\text{Ti} + ^{252}\text{Cf}$ .

**Table 3.5** The calculated values of fusion cross-sections and  $P_{\text{CN}}$  for  $^{48}\text{Ca} + ^{254}\text{Fm}$ .

# CONTENTS

CERTIFICATE

ACKNOWLEDGEMENT

ABSTRACT

LIST OF FIGURES

LIST OF TABLES

## CHAPTER 1

INTRODUCTION.....	11
1.1 ISLAND OF STABILITY.....	12
1.2 SUPERHEAVY NUCLEI.....	14
1.2.1 FUSION REACTIONS.....	15
1. COLD FUSION REACTIONS.....	16
2. HOT FUSION REACTIONS.....	17
1.3 ROLE OF DEFORMATIONS AND ORIENTATIONS.....	18
1.4 GENERAL PREDICTIONS FOR Z=119 AND Z=120.....	20
REFERENCES.....	22

## CHAPTER 2

2.1 METHODOLOGY.....	25
2.1.1 FUSION CROSS-SECTION USING PARTIAL WAVE ANALYSIS.....	25
2.1.2 THE FRAGMENTATION POTENTIAL.....	27
2.1.3 THE COULOMB POTENTIAL ( $V_C$ ).....	28
2.1.4 THE PROXIMITY POTENTIAL ( $V_P$ ).....	28

2.1.5 THE CENTRIFUGAL POTENTIAL ( $V_1$ ).....	29
REFERENCES.....	30
<b><u>CHAPTER 3</u></b>	
INTRODUCTION.....	32
RESULTS AND DISCUSSION.....	33
3.1 ANALYSIS OF DIFFERENT PROJECTILE-TARGET COMBINATIONS ON THE BASIS OF FUSION BARRIER.....	33
3.2 THE STUDY OF COLD VALLEY REGIONS OF $^{302}_{120}$ USING FRAGMENTATION POTENTIAL.....	38
SUMMARY AND CONCLUSIONS.....	42
REFERENCES.....	44

# **CHAPTER 1**

# CHAPTER 1

## INTRODUCTION

In the early 19<sup>th</sup> century, only 92 chemical elements from Hydrogen to Uranium were known to exist naturally out of which 83 are stable and 9 are radioactive. However, in the 1930s, the world of nuclear science began to discover new elements beyond Uranium i.e. Transuranics. Now the question comes that: How we can integrate our periodic table beyond naturally occurring Uranium? This occurs by the means of neutron capture followed by  $\beta$ -decays i.e. the neutrons are added to the elements and a new unstable isotope is formed which emits electrons via  $\beta$ -decay and changes to the next heavier element as shown in Fig. 1.1.

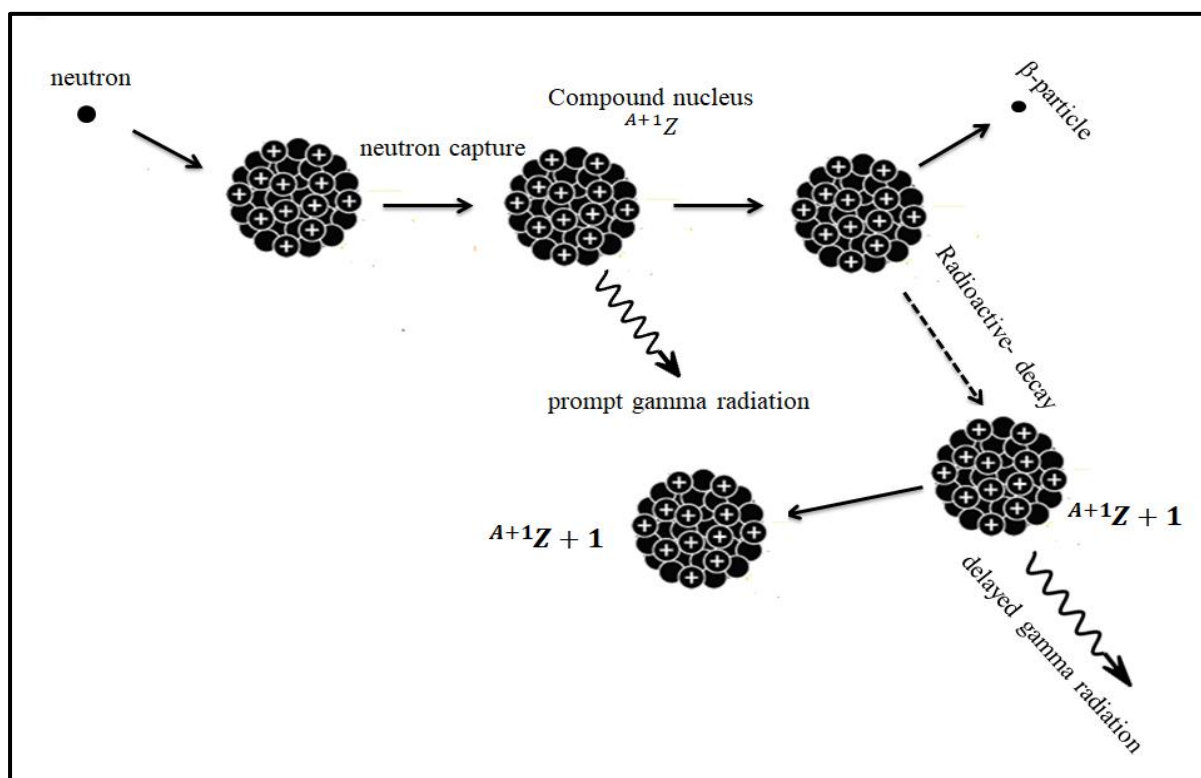


**Fig.1.1** Formation of a heavier nucleus via neutron capture followed by  $\beta$ -decay and  $\gamma$ - rays emission

After the production of transuranium elements, the synthesis of superheavy nuclei achieves significant progress in the era of nuclear physics. With the invention of new

generation accelerators heavy ions beams acceleration becomes possible that fuses with heavy elements to produce some super heavy ones. These new elements are not probably found in Nature at all but can be detected under precisely designed experiments using powerful nuclear tools as their life-time is very small [1-3]. During the synthesizing period of superheavy elements i.e. in the middle of 1930s, the phenomena known as nuclear fission came into picture, which needs an appropriate description and this lead to the discovery of Liquid Drop Model (Bohr and Wheeler in 1939) [4]. The Liquid Drop Model (LDM) is based on an assumption in which a nucleus is considered as a liquid drop. This model successfully explains the general characteristics of the nucleus and reproduces many collective properties. Importantly using this model, binding energies for wide range of nuclei were calculated, however it failed to explain the higher binding energies of the nuclei with magic numbers and thus it requires more microscopic description. Later in 1948, Shell model (SHM) [5-6], was discovered by the collaboration of several physicists, most notably Eugene Paul Wigner, Maria Goeppert Mayer and J. Hans D. Jensenis, which explains the magic numbers i.e. 2, 8, 20, 28, 50, 82 and the stability associated with them. According to this model, the nuclides with N or Z=2, 8, 20, 28, 50, 82 are more stable due to their filled shells. However, the doubly magic nuclei like  ${}^4_2\text{He}$ ,  ${}^{16}_8\text{O}$ ,  ${}^{40}_{20}\text{Ca}$ ,  ${}^{48}_{20}\text{Ca}$  as well as  ${}^{208}_{82}\text{Pb}$  attain extra stability and thus possess higher binding energies as compared to their neighboring nuclei. In the middle of 1960s, the concept of Macroscopic-Microscopic model was discovered by Strutinsky [7]. Using this model, the Binding energy is calculated as the sum of macroscopic part derived from LDM and as a correction term, a microscopic part derived from nuclear shell model. It is found as more accurate way to derive Binding energies of nuclei in contrast of using only LDM or SHM. The calculations of ground state binding energy provides the basic step to determine the stability of Superheavy Nuclei and hence, thereafter started a rush towards the synthesis of superheavy nuclei.

## 1.1 ISLAND OF STABILITY

The hypothesis of island of stability was given by G.T. Seaborg in late 1960s. It is based upon the nuclear shell model which states that like electrons in atomic shell, nucleons are also build up in nuclear shells. When the shells are completely filled, the Binding

energy per nucleon increases and nucleus achieves extra stability as compare to nearby nucleus. The Island of Stability is plotted as a function of N and Z which describes the yet not discovered isotopes of transuranium elements that are theorized to be much stable than others. The perspective offered by Shell Model leads to the discovery and stability of super heavy elements (SHE). Many theoretical studies have been carried out regarding the prediction and discovery of stability of SHE. In 1966, A. Sobiczewski *et. al.* [8] observed shell closure at  $Z=108$  and  $N=162$  for deformed nuclei and another at  $Z=114$  and  $N=184$  for spherical nuclei. These predictions based upon theoretical studies, have been further confirmed using various different approaches and finally it was observed that the shell closure lies at  $Z=114, 120, 126$  and  $N=172$  or  $184$ . These calculations indicate that the most stable superheavy nuclei in the center of 'island' could have large half-lives. The existence of an island of stability in the region of nuclei with  $Z=114$  and  $N=184$  caused the experimental investigation in the field of SHE. The interest is now further extended to next magic  $Z=120$ . Moreover, whether this magicity sustains for deformed nuclei [9-11].

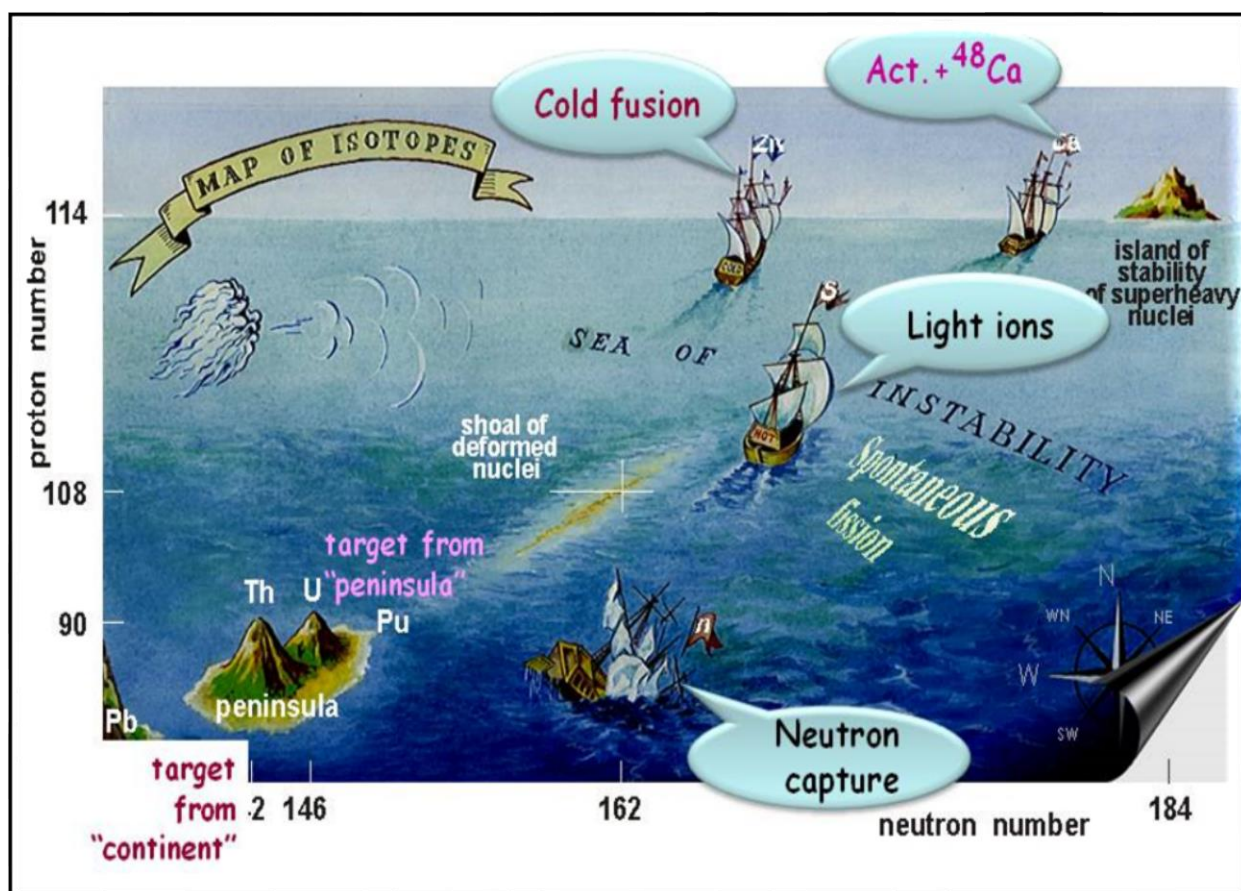


Fig.1.2 Island of Stability showing stabilities in super heavy region.

## 1.2 SUPERHEAVY NUCLEI

Superheavy elements are defined as the elements beyond the actinide series, beginning with Rutherfordium ( $Z=104$ ). As the technology advances, the discovery of Superheavy nuclei has started a race between America, Russia, and Germany. Brief descriptions of different superheavy nuclei are given below:

**Z=104-106 elements:** - The studies of these elements were carried out at Lawrence-Berkely laboratory and Joint Institute of Nuclear research (JINR) at Dubna. These elements were produced in the reactions induced by charged particles. The beam of  $^{12}\text{C}$ ,  $^{18}\text{O}$  or  $^{22}\text{Ne}$  is bombarded with the isotopes of Pu-Cf to obtain hot and rotating compound nucleus. Using this approach, the isotopes of  $Z=104-106$  elements were synthesized for the first time. The approved names for  $Z=104$ , 105 and 106 by International Union of Pure and Applied Chemistry (IUPAC) are Rutherfordium (Rf), Dubnium (Db) and Seaborgium (Sg) respectively.

**Z=107-112 elements:** - The experiments for the production and investigation of elements beyond  $Z=106$  were performed after the discovery of “Cold fusion” (discussed in next section) reaction by Oganesson *et. al.*[12]. In these reactions, magic target nuclei  $^{208}\text{Pb}$  or  $^{209}\text{Bi}$  collide with massive projectile with  $A \geq 40$ , forming a compound nucleus. The elements with  $Z=107-112$  have been synthesized using Cold-fusion reactions at SHIP (Separator for Heavy Ion reaction Products is an electromagnetic separator which has been designed for the synthesis and investigation of superheavy elements) using massive ions  $^{54}\text{Cr}$ ,  $^{58}\text{Fe}$  and  $^{70}\text{Zn}$ . The names of these nuclei accepted by International Union of Pure and Applied Chemistry (IUPAC) are given below:

- 1)  $Z=107$  Bohrium (Bh) in 1997.
- 2)  $Z=108$  Hassium (Hs) in 1997.
- 3)  $Z=109$  Meitnerium (Mt) in 1997.
- 4)  $Z=110$  Darmstadtium (Ds) in 2003.
- 5)  $Z=111$  Roentgenium (Rg) in 2004.
- 6)  $Z=112$  Copernicium (Cn) in 2010.

**Z=113-118 elements:** - For the synthesis of superheavy nuclei from  $Z=113-118$ , “Hot-fusion” reactions (discussed in next section) were used in contrast to cold fusion reactions.

The neutron-rich isotopes of transuranium elements were bombarded with  $^{48}\text{Ca}$ -projectile and were well made at Flerov Laboratory for Nuclear Reactions (FLNR). The proposed names by International Union of Pure and Applied Chemistry (IUPAC) are given below:

- 1) Z=113 Nihonium (Nh) on 28 November 2016.
- 2) Z=114 Flerovium (Fl) on 30 May 2012.
- 3) Z=115 Moscovium (Mc) on 28 November 2016.
- 4) Z=116 Livermorium (Lv) on May 30, 2012.
- 5) Z=117 Tennessine (Ts) in November 2016.
- 6) Z=118 Oganesson (Og) on 28 November 2016.

### 1.2.1 Fusion reactions

Heavy ion fusion reactions have been widely used for the synthesis of heavy and superheavy elements. Apparently, the complete fusion reactions have received the greatest attention in connection with stability and synthesis of superheavy nuclei. A complete fusion is a process when the heavy projectile fuses with the heavier target. During the process, the mutual repulsion of protons due to higher  $Z_1Z_2$  product competes with the fusion process, but the quantum mechanical effects entice nucleons to fill the magic shells and lend some extra stability. This will lead to the formation of completely fused system with a reduced probability of survival against fission.

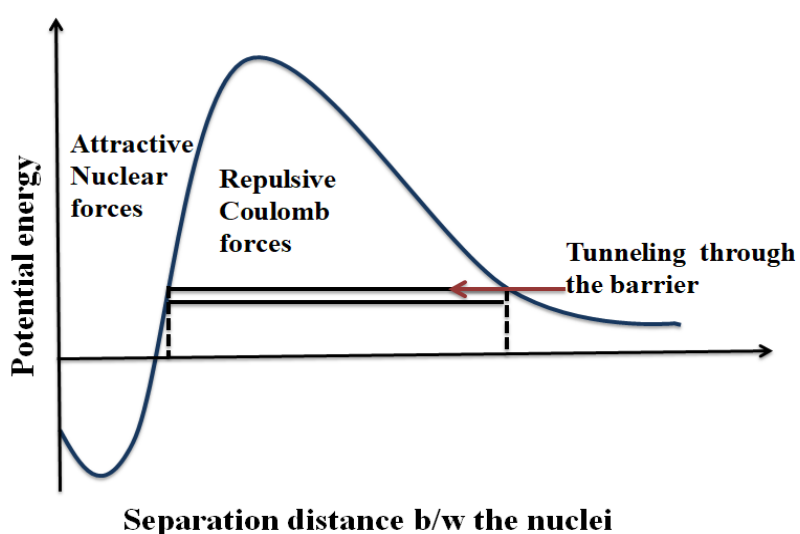


**Fig.1.3** Potential Barrier v/s the separation distance between the nuclei

Till now, significant progress has been achieved in experimental and theoretical field regarding the investigation of superheavy nuclei. To extend the periodic table two different approaches have been used:

- Cold fusion reactions were mainly performed at GSI, Darmstadt and RIKEN, Japan. Using cold fusion reaction, elements Z=107-112 were synthesized.
- Another one is, Hot fusion reactions which lead to the discovery of Z=113-118 Superheavy elements.

The details about cold and hot fusion reaction are given as:

**1. COLD FUSION REACTIONS:** - The concept of cold fusion for the synthesis of superheavy nuclei was given by Oganessian *et. al.* [12]. In this reaction, strongly bound target nuclei i.e.  $^{208}\text{Pb}$  or  $^{209}\text{Bi}$  fuse with isotopes of elements from Cr to Zn, resulting in the formation of Compound nucleus. Cold fusion reactions refer to the one with lowest barrier and highest separation distance (i.e. elongated configuration). The compound nucleus formed has low excitation energy i.e. only 12-20 MeV and thus the evaporation of one neutron is sufficient to prevent the fission which is the main advantage of using cold fusion [13-20].

Sr. No.	Atomic No.	Element	Reaction
1)	107	Bohrium(Bh)	$^{209}_{83}\text{Bi} + ^{54}_{24}\text{Cr} \rightarrow ^{262}_{107}\text{Bh} + n$
2)	108	Hassium(Hs)	$^{208}_{82}\text{Pb} + ^{58}_{26}\text{Fe} \rightarrow ^{265}_{108}\text{Hs} + n$
3)	109	Mietnerium(Mt)	$^{209}_{83}\text{Bi} + ^{58}_{26}\text{Fe} \rightarrow ^{266}_{109}\text{Mt} + n$
4)	110	Darmstatium(Ds)	$^{208}_{82}\text{Pb} + ^{62}_{28}\text{Ni} \rightarrow ^{269}_{110}\text{Ds} + n$
5)	111	Roentgenium(Rg)	$^{209}_{83}\text{Bi} + ^{64}_{28}\text{Ni} \rightarrow ^{272}_{111}\text{Rg} + n$
6)	112	Copernicium(Cn)	$^{208}_{82}\text{Pb} + ^{70}_{30}\text{Zn} \rightarrow ^{277}_{112}\text{Cn} + n$

**Table 1.1** Elements synthesized via Cold fusion [21].

But unfortunately, this method is not applicable when moving to the domain of spherical shells Z=114 and N=184. The synthesis of heavier nuclei is achieved by increasing the atomic number of projectile. This causes an increase in Coulomb repulsions and decrease in

the probability of compound nucleus formation. Thus to reach the effect of N=184, it is necessary to increase the number of neutrons in compound nucleus. Hence, the approach to synthesize super heavy elements beyond Z=112 changed from “Cold fusion reaction” to “Hot fusion reaction” [15].

**2. HOT FUSION REACTIONS:** - For the next heavier elements, the adoption of asymmetric target-projectile combinations provides better option to demolish the Coulomb repulsion effect. Hot fusion reactions refer to the one with highest barrier and lowest separation distance (i.e. compact configuration). The fusion of actinide targets with  $^{48}\text{Ca}$  beams gives more neutron-rich and stable nuclei. This fusion generates a compound nucleus with excitation energy of 40-50MeV. However, the evaporation of four or five neutrons reduces the excitation energy of compound nucleus below fission barrier. The list of the elements created via hot fusion from Z=113-118 at Joint Institute of Nuclear Research, JINR in Dubna [13-20].

Sr. No.	Atomic No.	Element	Reaction
1.	113	Nihonium (Nh)	$^{249}_{98}\text{Am} + ^{48}_{20}\text{Ca} \rightarrow ^{288}_{115} + 3\text{n} \rightarrow ^{284}_{113} + \alpha$
2.	114	Flerovium (Fl)	$^{244}_{94}\text{Pu} + ^{48}_{20}\text{Ca} \rightarrow ^{292}_{114}\text{Fl}^* \rightarrow ^{289}_{114}\text{Fl} + 3\text{n}$
3.	115	Moscovium (Mc)	$^{243}_{95}\text{Am} + ^{48}_{20}\text{Ca} \rightarrow ^{288}_{115}\text{Uup} + 3^1_0\text{n}$
4.	116	Livermorium (Lv)	$^{248}_{96}\text{Cm} + ^{48}_{20}\text{Ca} \rightarrow ^{296}_{116}\text{Lv}^* \rightarrow ^{293}_{116}\text{Lv} + 3\text{n}$
5.	117	Tennesine (Ts)	$^{249}_{97}\text{Bk} + ^{48}_{20}\text{Ca} \rightarrow ^{297}_{117}\text{Uus}^* \rightarrow ^{293}_{117}\text{Uus} + 4\text{n}$
6.	118	Oganesson (Og)	$^{249}_{98}\text{Cf} + ^{48}_{20}\text{Ca} \rightarrow ^{294}_{118}\text{Uuo} + 3\text{n}$

**Table 1.2** Elements synthesized via hot fusion [22].

Going above 118 presents new challenges. Calcium-48 doesn't provide enough protons for the job. Therefore, heavier projectile such as titanium and chromium could serve as prime

candidates. This needs further investigation for economical synthesis of long-life element with  $Z=120$ .

### 1.3 ROLE OF DEFORMATIONS AND ORIENTATIONS

Most of the nuclei with completely filled shells are relatively stable and are spherical in shape but some can lower their energy by rearranging their protons and neutrons and acquiring deformed shapes i.e. the non-spherical charge distribution. A number of calculations were made which all resulted in showing that the fusion barrier is lowered due to deformations and orientations of the colliding nuclei. The nuclei mainly include quadrupole, octupole and hexadecapole deformations but results from higher multipole deformations are not always favorable for fusion. Therefore, in the present study we are confined with quadrupole deformations only. The following Fig. 1.4 below gives the comparison of charge distribution between a spherical nucleus in Fig. 1.4(a) and a quadrupolar nucleus in Fig. 1.4(b).

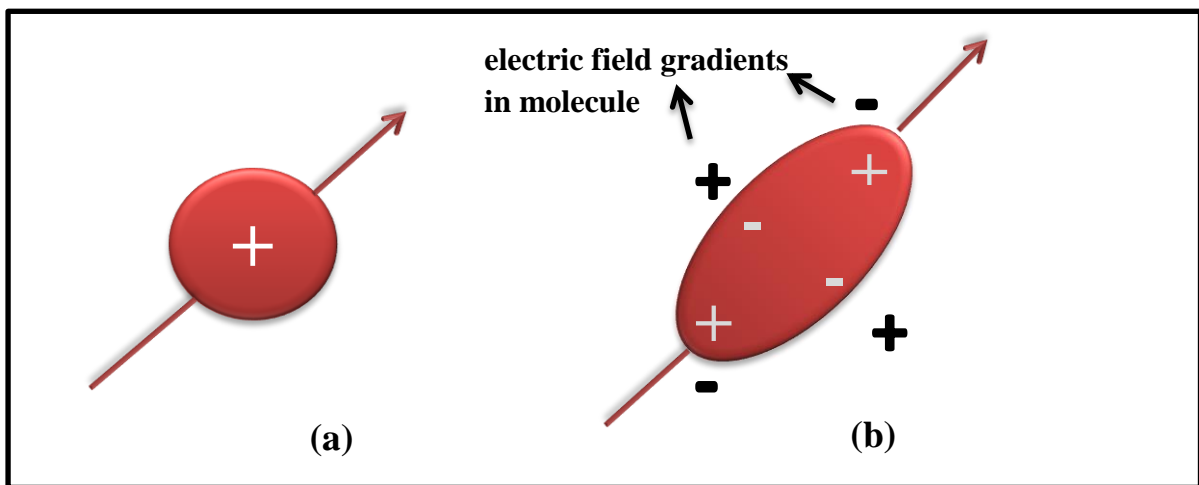


**Fig.1.4** Nuclear charge distribution in (a) spherical and (b) deformed case.

The quadrupole deformations ( $\beta_2$ ) are governed by the electric quadrupole moment  $Q$  i.e. when

- i.  $Q=0$ , it symbolizes spherically symmetric case as shown in above figure 1.4 (a).
- ii.  $Q=+ve$ , then this indicate prolate shape.

iii.  $Q = -ve$ , then this indicates oblate shape.

The shapes of nucleus with quadrupole deformations are shown below:

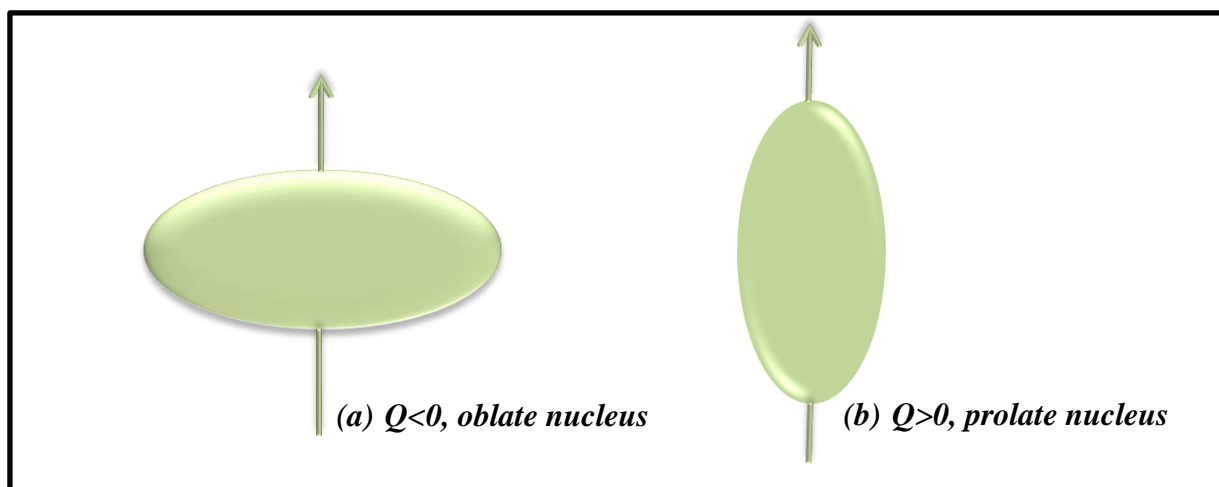


**Fig.1.5** (a) and (b) describes the *Quadrupole deformed shapes of a nucleus*.

Along with the deformations, the orientations of nucleus also plays equally important role in the reaction analysis. In many theoretical observations, it has been accounted that the barrier height is lowered for pole-to-pole or nose-to-nose configuration of deformed nuclei. As it offers large separation distance and hence reduces the interaction barrier, since ( $V_T \propto 1/R$ ).

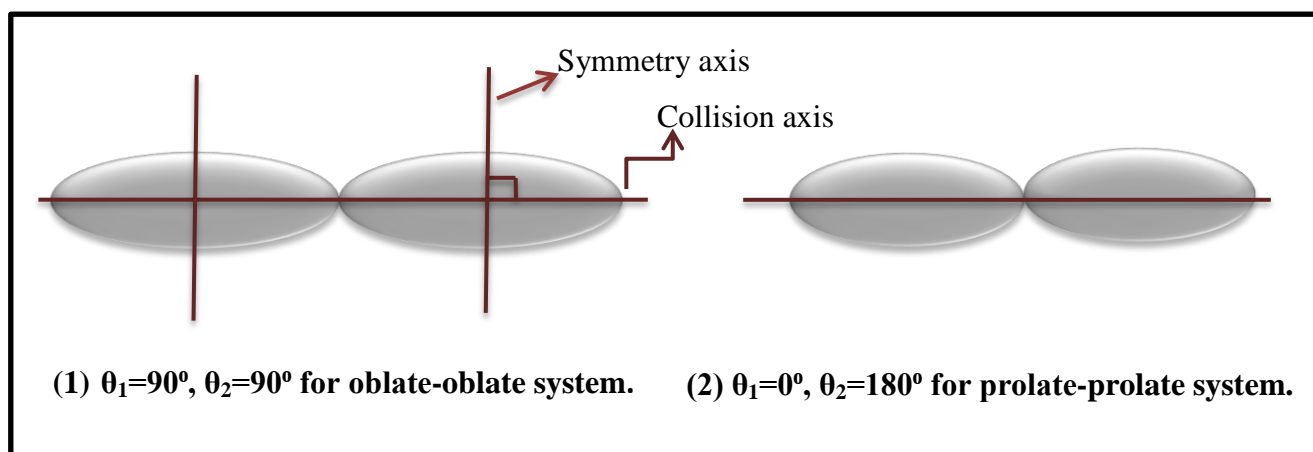


**Fig.1.6** Systematic diagram of quadrupolar nuclei with optimized orientations for “cold, elongated” configurations.

This type of configurations of deformed nuclei refers to “cold, elongated configuration”. Another type of configuration is known as “hot, compact configuration”, which refers the small interaction radius and highest barrier to the colliding nuclei. The systematic diagram of ‘compact configuration’ is shown below:

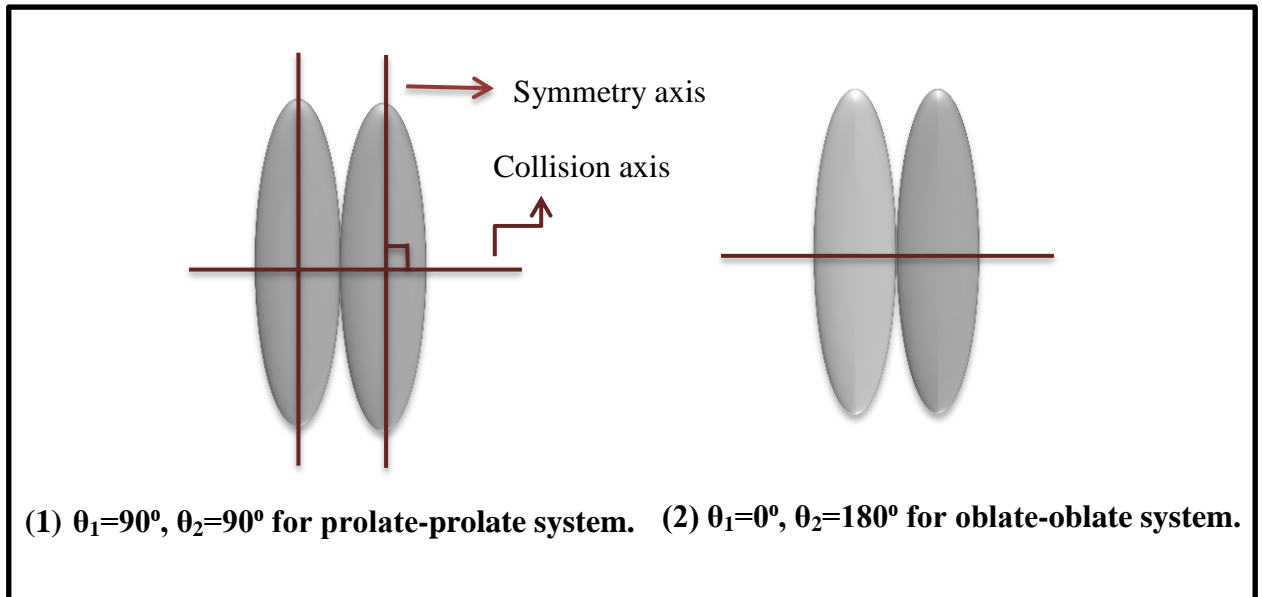


**Fig.1.7** Systematic diagram of quadrupolar nuclei with optimized orientations along “hot, compact” configurations.

Thus, in order to have meaningful predictions for the synthesis of superheavy nuclei, it is important to include deformations and orientations effect into consideration. In the present work, optimum configurations are employed [23-27].

## 1.4 GENERAL PREDICTIONS FOR Z=119 and 120

With the synthesis of Z=118, the seventh row of our periodic table is now complete, but this is not the end. Attempts are being made by researchers for the next heavier ones in the hope to reach the next “island of stability” i.e. Z=120 in place of 114.

In the search of next island of stability Z=120, till now many reactions have been chosen by the researchers and our motive is to predict the best out of these. The increased fusion cross-

section of superheavy nuclei gives the direct signal towards the nuclear shell effects, probably with  $Z=120$  and  $N=184$  and based on these cross-sections, we can pick up a set of reactions for our work. For  $Z>112$ , it becomes difficult to produce heavier nuclei via cold fusion reaction. Therefore, the  $^{48}\text{Ca}$ -based hot fusion reactions are considered. In hot fusion reactions with  $^{48}\text{Ca}$ -projectile, the choice for actinide target is *Es* ( $Z=99$ ) and *Fm* ( $Z=100$ ), for the compound nucleus  $Z=119$  and  $120$  to get synthesized respectively. However, particularly for the nuclei  $Z>118$ , the  $^{48}\text{Ca}$  can't be use as a prime candidate, since it doesn't provide enough number of protons. However, Einsteinium (*Es*,  $Z=99$ ) as the having half-life 276 days, is sufficient to be used as a target. But it's impossible to accumulate sufficient amount of this matter to prepare a target. Also, the Californium (*Cf*,  $Z=98$ ) is the heaviest available target that can be used in the experiments. Thus, the more realistic way is to shift towards the elements heavier than  $^{48}\text{Ca}$  projectile. Hence, heavier projectile such as Titanium and Chromium beams seems to be more promising for the further synthesis of superheavy nuclei. The present experimental status of superheavy element research by GSI (Germany) has predicted largest production rate for the more mass asymmetric projectile-target combination  $^{54}\text{Cr} + ^{248}\text{Cm}$  among the reactions  $^{58}\text{Fe} + ^{244}\text{Pu}$  and  $^{64}\text{Ni} + ^{238}\text{U}$  for  $Z=120$ . Besides the  $^{48}\text{Ca}$  and  $^{54}\text{Cr}$  projectile,  $^{50}\text{Ti}$  beam could also serve to be the most applicable for the production of more heavier elements, providing more mass asymmetry and thus  $^{50}\text{Ti} + ^{249}\text{Bk}$  [28] for  $Z=119$  and  $^{50}\text{Ti} + ^{249}\text{Cf}$  [29] and  $^{50}\text{Ti} + ^{252}\text{Cf}$  [30] for  $Z=120$ , projectile-target combinations are of more interest. The study of superheavy  $Z=120$  is of great interest because it is useful in determining whether the magic proton shell closure would remain be at  $Z=114$  or at higher proton number  $Z=120$  or  $126$  and also it is experimentally observed that even-even nuclei are easier to synthesize than odd-odd nuclei, that's why we are very much interested in the synthesis of  $Z=120$  [31].

The aim of the present work, is to study the synthesis of superheavy nucleus  $Z=120$  using the chosen projectile-target combinations i.e.  $^{54}\text{Cr} + ^{248}\text{Cm}$ ,  $^{50}\text{Ti} + ^{249}\text{Cf}$ ,  $^{50}\text{Ti} + ^{252}\text{Cf}$ ,  $^{48}\text{Ca} + ^{254}\text{Fm}$ , along with the role of deformations and orientations in their synthesization process. The analysis is done with the framework of Wong formula described briefly in next chapter. Some new target-projectile combinations will also be predicted from the cold valleys in the fragmentation potential of decaying  $^{302}120$  elements.

## REFERENCES

- [1] S. Hofmann, J. Phys. G. Nucl. Part. Phys. 42, 114001 (2015).
- [2] M. Schädel, *The Chemistry of Superheavy Elements*, (US Springer) (Book) (2003).
- [3] S. Hofmann, *On beyond Uranium: Journey to the end of the Periodic Table*, (Taylor & Francis e-Library) (Book) (2003).
- [4] N. Bohr and J. A. Wheeler, Phys. Rev. 56, 426 (1939).
- [5] M. G. Mayer, Phys. Rev. 74, 235 (1948).
- [6] M. G. Mayer, Phys. Rev. 75, 1969 (1949).
- [7] V. M. Strutinsky, Nucl. Phys. A 95, pp. 420-442 (1967).
- [8] A. Sobiczewski *et.al.* Phys. Lett. 22, 500 (1966).
- [9] R. K. Gupta, S. K. Patra and W. Grenier, Mod. Phys. Lett. A, 12, 1727 (1997).
- [10] K. Rutz, M. Bender, T. Burvenich, T. Schilling, Phys. Rev. C 56, 238 (1997).
- [11] A. T. Kruppa, M. Bender, W. Nazarewicz, P. G. Reinhard, T. Vertse and S. Cwiok, Phys. Rev. C 61, 034313 (2000).
- [12] J. H. Hamilton, S. Hofmann, and Y. T. Oganessian, Annu. Rev. Nucl. Part. Sci. 63, 383-405 (2013).
- [13] S. Hofmann, Rep. Prog. Phys. 61, 639 (1995).
- [14] S. Hofmann and G. Munzenberg, Rev. Mod. Phys. 72, 733 (2000).
- [15] V. Zagrebaev and W. Greiner, Phys. Rev. C 78, 034610 (2008).
- [16] S. Hofmann *et.al.*, Nucl. Phys. A 734, 93 (2004).
- [17] V. I. Zagrebaev, A. V. Karpov, and W. Greiner, Phys. Rev. C 85, 014608 (2012).
- [18] Y. Nagame, H. Haba, Journal of Nuclear and Radiochemical Sciences 6, 3 pp.205-210, (2005).

- [19] Yu. Ts. Oganessian, Phys. Rev. Lett. 109, 162501 (2012).
- [20] Yu. Ts. Oganessian, Phys. Rev. Lett. 108, 022502 (2012).
- [21] S. Hofmann and G. Munzenberg, Rev. Mod. Phys. 72, 3 (2000).
- [22] Y. Oganessian, J. Phys. G: Nucl. Part. Phys. 34, 165 (2007).
- [23] K. S. Krane, *Introductory Nuclear Physics*, (Wiley) (Book) (1998).
- [24] V. I. Zagrebaev, Y. Aritomo, M. G. Itkis and Yu. Ts. Oganessian, Phys. Rev. C 65, 014607 (2001).
- [25] M. Manhas and R. K. Gupta, Phys. Rev. C 72, 024606 (2005).
- [26] R. K. Gupta, N. Singh and M. Manhas, Phys. Rev. C 70, 034608 (2004).
- [27] V. Yu. Denisov and N. A. Pilipenko, Phys. Rev. C 76, 014602 (2007).
- [28] L. Zhu, W. J. Xie and F. S. Zhang, Phys. Rev. C 89, 024615 (2014).
- [29] A. K. Nasirov, G. Mandaglio, G. Giardina, A. Sobiczewski, and A. I. Muminov, Phys. Rev. C 84, 044612 (2011).
- [30] Z. H. Liu and J. D. Bao, Phys. Rev. C 80, 054608 (2009).
- [31] R. Kumar, K. Sandhu, M. K. Sharma and R. K. Gupta, Phys. Rev. C 87, 054610 (2013).

# **CHAPTER 2**

## **CHAPTER 2**

### **2.1 METHODOLOGY**

In the fusion process, the first stage is the capture of projectile by target nuclei, forming di-nuclear structure after the full momentum transfer of colliding nuclei into shape deformation, excitation energy and rotational energy. For the capture process, the projectile must have sufficient initial energy to overcome the interaction barrier formed by repulsive Coulomb potential and Centrifugal potential along with attractive nuclear potential. The capture cross-section are calculated using the Wong formula [1-3]. However, the complete fusion cross-section for a superheavy nucleus is described as the product of capture cross-section and the probability of compound nucleus formation  $P_{CN}$  described in section 2.1.1.

In the prediction of Superheavy nuclei, the fragmentation potential is an important tool. As it provides useful information regarding the favorable target-projectile combinations, where fragmentation potential is expressed as the sum of the binding energies and total interaction potential. The total interaction potential is described along with various interaction potential such as Coulomb potential, proximity potential and centrifugal potential in section 2.1.2, 2.1.3, 2.1.4, 2.1.5 respectively. The different target-projectile combinations with low fragmentation potential refer to the most favorable case in the synthesis of superheavy nuclei. Unlike the total interaction potential, the fragmentation potential is calculated in terms of mass-asymmetry co-ordinate  $\eta$  defined as  $\eta = \frac{A_1 - A_2}{A_1 + A_2}$ , where  $A_1$  and  $A_2$  are masses of projectile and target nuclei.

#### **2.1.1 FUSION CROSS-SECTION USING PARTIAL WAVE ANALYSIS**

The fusion cross-section of two deformed and oriented nuclei, inclined at an angle  $\theta_i$  at center of mass energy  $E_{cm}$  is calculated using partial wave analysis [3], as

$$\sigma(E_{cm}, \theta_i) = \sum_{\ell=0}^{\infty} \sigma_{\ell} = \frac{\pi}{k^2} \sum_{\ell=0}^{\infty} (2\ell + 1) P_{\ell}(E_{cm}, \theta_i) \quad (2.1)$$

where  $k = \sqrt{\frac{2\mu E_{cm}}{\hbar^2}}$ ,  $\mu$  is reduced mass and

$$P_\ell = \left[ 1 + \exp \left( 2\pi \left( \frac{V_B^\ell - E_{cm}}{\hbar\omega_\ell} \right) \right) \right]^{-1} \quad (2.2)$$

is the penetration probability which is estimated in terms of barrier height  $V_B^\ell$  and curvature  $\hbar\omega_\ell$  using Hill Wheeler approximation [4]. The total interaction potential barrier  $V_T^\ell(\mathbf{R})$  with deformations and orientations is defined as

$$V_T^\ell(\mathbf{R}) = V_c(\mathbf{R}, Z_i, \beta_{\lambda i}, \theta_i, T) + V_N(\mathbf{R}, A_i, \beta_{\lambda i}, \theta_i, T) + V_\ell(\mathbf{R}, A_i, \beta_{\lambda i}, \theta_i, T) \quad (2.3)$$

The detailed study of each term is discussed in sec 2.1.2.

Using equation (2.2) in equation (2.1) and replacing  $\ell$ -summation by integral, giving  $\ell=0$  base Wong formula, barrier characteristics ( $V_B$ ,  $\hbar\omega$  and  $R_B$ )

$$\sigma(E_{cm}, \theta_i) = \frac{R_B^2}{2E_{cm}} \ln \left\{ 1 + \exp \left( \frac{2\pi}{\hbar\omega_0} (E_{cm} - V_B^0) \right) \right\} \quad (2.4)$$

under following conditions:

- i.  $\hbar\omega_\ell \approx \hbar\omega_0$
- ii.  $V_B^\ell \approx V_B^0 + \frac{\hbar^2 \ell(\ell+1)}{2\mu R_B^2}$ , which means to assume  $R_B^\ell \approx R_B^0$ .

The Wong formula in equation (2.4) is applicable for spherical partners of colliding nuclei. However when deformations are included, the equation is replaced by

$$\sigma(E_{cm}) = \int_{\theta_1, \theta_2=0}^{\pi/2} \sigma(E_{cm}, \theta_1, \theta_2) \sin \theta_1 d\theta_1 \sin \theta_2 d\theta_2 \quad (2.5)$$

In case of light, medium or heavy nuclei, total fusion cross-section are calculated using Wong formula, with an assumption that  $\sigma_{fus} = \sigma_{capture}$ . As we are concerned with the study of superheavy nuclei, the probability of compound nucleus formation decreases gradually with increase in atomic mass. Therefore, in the case of superheavy nucleus, the total fusion cross-section is given as

$$\sigma_{fus} = \sigma_{capture} \times P_{CN} \quad (2.6)$$

Where,  $P_{CN}$  is the probability of the formation of the completely fused compound nucleus from the di-nuclear system after the capture stage. The energy dependent  $P_{CN}$  is given as:

$$P_{CN} = \frac{\exp(-c(\chi_{eff} - \chi_{thr}))}{1 + \exp\left(\frac{V_B^* - V^*}{\Delta}\right)} \quad (2.7)$$

where,  $V^*$  is the excitation energy of compound nucleus,  $V_B^*$  is the excitation energy of Compound nucleus at  $E_{cm} \approx$  coulomb barrier and  $\Delta \approx 4 \text{ MeV}$  is an adjustable parameter and  $\chi_{eff}$  is the effective fissility given as

$$\chi_{eff} = \left[ \frac{Z^2/A}{(Z^2/A)_{crit}} \right] (1 - \alpha + \alpha f(k)) \quad (2.8)$$

$$\text{where, } \left( \frac{Z^2}{A} \right)_{crit} = 50.883 \left[ 1 - 1.7826 \left( \left( \frac{N-Z}{A} \right) \right)^2 \right], \quad (2.9)$$

$$f(k) = \frac{4}{k^2 + k + \frac{1}{k} + \frac{1}{k^2}}, \quad (2.10)$$

$$\text{and } k = \left( \frac{A_1}{A_2} \right)^{1/3} \quad (2.11)$$

where,  $Z$  is atomic number,  $A$  is mass number and  $N$  is neutron number of the compound nucleus formed.  $A_1$  is the projectile mass and  $A_2$  is target mass. As suggested by Loveland [5], the best fit for hot fusion reaction is:

- i. If  $\chi_{eff} \leq 0.80$ , then  $c = 104$  and  $\chi_{thr} = 0.69$ .
- ii. If  $\chi_{eff} \geq 0.80$ , then  $c = 82$  and  $\chi_{thr} = 0.69$ .

Using equation (2.7) in equation (2.6), the total fusion cross-sections of chosen reactions are predicted at energies well below and above the coulomb barrier [6].

## 2.1.2 THE FRAGMENTATION POTENTIAL

The fragmentation potential is defined as the sum of the binding energies and total interaction potential stated in equation (2.3) and the temperature-dependent fragmentation potential for the two deformed ( $\beta_{\lambda i}$ ) oriented at  $\theta_i$  is [7]

$$V(\eta, R, \ell, T) = - \sum_{i=1}^2 B_i(Z_i, \beta_{\lambda i}, A_i, T) + V_c(R, Z_i, \beta_{\lambda i}, \theta_i, T) + V_p(R, A_i, \beta_{\lambda i}, \theta_i, T) + V_\ell(R, A_i, \beta_{\lambda i}, \theta_i, T) \quad (2.12)$$

$\mathbf{R}$  is the relative separation distance and  $\mathbf{B}_i$  is the Binding energies, taken from the calculations of Moller *et. al.* [8] and from experiments [9].

### 2.1.3 THE COULOMB POTENTIAL ( $V_C$ )

It describes the presence of the repulsive forces b/w the interacting nuclei. The Coulomb potential for the two interacting hot-deformed and oriented nuclei [10-11] is given as:

$$V_c(\mathbf{R}, \mathbf{Z}_i, \beta_{\lambda i}, \theta_i, T) = \frac{Z_1 Z_2 e^2}{R(T)} + 3 Z_1 Z_2 e^2 \sum_{\lambda, i=1,2} \frac{R_i^{\lambda}(\alpha_i, T)}{(2\lambda+1)R(T)^{\lambda+1}} Y_{\lambda}^{(0)}(\theta_i) \left[ \beta_{\lambda i} + \frac{4}{7} \beta_{\lambda i}^2 Y_{\lambda}^{(0)}(\theta_i) \right] \quad (2.13)$$

where,  $Y_{\lambda}^{(0)}$  is a spherical harmonics function and  $\mathbf{R}_i$  is the radius vector given as:

$$\mathbf{R}_i(\alpha_i, T) = R_{0i}(T) \left[ \mathbf{1} + \sum_{\lambda} \beta_{\lambda i} Y_{\lambda}^{(0)}(\alpha_i) \right] \quad (2.14)$$

and

$$R_{0i}(T) = \left[ 1.28 A_i^{1/3} - 0.76 + 0.8 A_i^{-1/3} \right] \times (1 + 0.0007 T^2) \quad (2.15)$$

### 2.1.4 THE PROXIMITY POTENTIAL ( $V_P$ )

The potential that arises within a small distance ( $\approx 2fm$ ) between the two nuclei at the time of interaction. In the present work, we have used Blocki's pocket formula for understanding the reaction dynamics of super heavy elements. The nuclear proximity potential for deformed and oriented nuclei (temperature-dependent) [12-13] is:

$$V_P(s_0(T)) = 4\pi \bar{R} \gamma b(T) \phi(s_0(T)) \quad (2.16)$$

where,  $s_0$  is the shortest separation distance between the interacting nuclei and  $\gamma$  is the surface energy constant.

$$\gamma = 0.9517 \left[ 1 - 1.7826 \left( \frac{N-Z}{A} \right)^2 \right] \quad (2.17)$$

$\phi(s_0)$  is universal function, independent of geometry and shapes of nuclear system, but depends on the minimum separation distance  $s_0$  given as:

i. for  $s_0 \leq 1.2511$ ,  $\phi(s_0) = -\frac{1}{2}(s_0 - 2.54)^2 - 0.0852(s_0 - 2.54)^3$

ii. for  $s_0 \geq 1.2511$ ,  $\phi(s_0) = -3.437 \exp\left(-\frac{s_0}{0.75}\right)$ ,

$b$  is the nuclear surface thickness, given as

$$\mathbf{b}(T) = 0.99(1 + 0.009T^2) \quad (2.18)$$

and  $\bar{R}$  is the mean curvature radius.

### 2.1.5 THE CENTRIFUGAL POTENTIAL ( $V_\ell$ )

The rotational motion gives an additional energy due to the angular momentum is defined [14] as:

$$V_\ell(R, A_i, \beta_{\lambda i}, \theta_i, T) = \frac{\hbar^2 \ell(\ell+1)}{2I(T)} \quad (2.19)$$

where,  $I$  is the moment of inertia and is defined as:

i. In complete sticking limit,

$$I_s(T) = \mu R^2 + \frac{2}{5} A_1 m(R_1^2)(\alpha_1, T) + \frac{2}{5} A_2 m(R_2^2)(\alpha_2, T) \quad (2.20)$$

ii. In Non-sticking limit,

$$I_{Ns}(T) = \mu R^2 \quad (2.21)$$

where,  $\mu = \left( \frac{A_1 A_2}{A_1 + A_2} \right)$ , is reduced mass and is nucleon mass.

## REFERENCES

- [1] C. Y. Wong, Phys. Rev. Lett. 31, 766 (1973).
- [2] R. Kumar, M. Bansal, S. K. Arun and R. K. Gupta, Phys. Rev. C 80, 034618 (2009).
- [3] Rajni, R. Kumar and M. K. Sharma, Phys. Rev. C 90, 044604 (2014).
- [4] D. L. Hill and J. A. Wheeler, Phys. Rev. 89, 1102 (1953).
- [5] W. Loveland, Phys. Rev C 76, 014612 (2007).
- [6] K. P. Santhosh and V. Safoora, Phys. Rev. C 94, 024623 (2016).
- [7] R. K. Gupta, M. Manhas, G. Munzenberg and W. Greiner, Phys. Rev. C 72, 014607 (2005).
- [8] P. Moller *et. al.*, At. Data Nucl. Data Tables 59, 185 (1995).
- [9] G. Audi and A. H. Wapstra, Nucl. Phys. A 4, 595 (1995).
- [10] R. K. Gupta, M. Balasubramaniam, R. Kumar, N. Singh, M. Manhas and W. Greiner, J. Phys. G: Nucl. Part. Phys. 31, 766 (1973).
- [11] G. Royer and J. Migner, J. Phy. G 18, 1781 (1992).
- [12] J. Blocki, J. Randrup, W. J. Swiatecki, and C.F. Tsang, Ann. Phys. 105, 427 (1977).
- [13] R. K. Gupta, N. Singh and M. Manhas, Phys. Rev. C 70, 034608 (2004).
- [14] R. Kumar, K. Sandhu, M. K. Sharma and R. K. Gupta, Phys. Rev. C 87, 054610 (2013).

# **CHAPTER 3**

## **CHAPTER 3**

### **INTRODUCTION**

In the present work, different calculations are done for four different chosen entrance channels or combinations i.e.,  $^{54}\text{Cr} + ^{248}\text{Cm}$  [1],  $^{50}\text{Ti} + ^{249}\text{Cf}$  [1],  $^{48}\text{Ca} + ^{254}\text{Fm}$  and  $^{50}\text{Ti} + ^{252}\text{Cf}$  [2], while taking the effects of quadrupole deformations with the corresponding optimum orientations along collision axis for “hot, compact” configurations, since they have significant effect on the interaction potential which consequently modifies the fusion cross-section (described in detail in Chapter 2) and could serve our purpose more effectively (as discussed in Chapter 1 already).

The present work is divided into parts: Firstly the fusion cross-sections are calculated for some earlier predicted reactions using Wong formula and Secondly, using the Fragmentation potential, new combinations are predicted. We calculated the fusion barrier which is related to the hindrance that the projectile must need to overcome in order to get completely fused with the target. Then the fusion cross-sections as a product of capture cross-sections and probability of the formation of compound nucleus are calculated for the chosen reactions i.e.  $^{54}\text{Cr} + ^{248}\text{Cm}$ ,  $^{50}\text{Ti} + ^{252}\text{Cf}$ ,  $^{48}\text{Ca} + ^{254}\text{Fm}$  leads to  $^{302}_{120}$  and  $^{50}\text{Ti} + ^{249}\text{Cf}$  giving  $^{299}_{120}$ . The calculations are made using Wong formula and then the results are compared. After that, fragmentation potential is plotted against fragment mass ( $A_2$ ), which consequently helps to predict another target-projectile combinations from their deep minima's also known as cold reaction valley i.e. the combinations with greater probabilities. Further for these new combinations, the interaction potential is plotted against the separation distance  $R$  (fm) in order to examine the suitable combination that could be used for the synthesis of  $Z=120$  with lower barrier.

## RESULTS AND DISCUSSIONS

### 3.1 Analysis of Different projectile-target combinations on the basis of Fusion Barrier

In the synthesis of superheavy elements, heavy projectile-target needs to fuse together, but this increase the Coulomb interactions and hence reduce the formation probability of superheavy nuclei. In order to overcome the fusion anomalies, mass asymmetric reactions seems to be more favorable. According to earlier studies [3], “Hot-fusion reactions” using  $^{48}\text{Ca}$ -projectile is always considered as the first choice for the formation of superheavy elements for  $Z \geq 113$ . But for the production of  $Z=119$  and  $120$ , since Ca-projectile doesn't provide enough number of protons with the heaviest available target Californium (Cf) with  $Z=98$ , therefore more asymmetric projectile-target combinations are needed to be explored. Recently, A. K. Nasirov *et. al.* [1], suggested  $^{54}\text{Cr} + ^{248}\text{Cm}$  and  $^{50}\text{Ti} + ^{249}\text{Cf}$  and Z. H. Liu *et.al.* [2], suggested  $^{50}\text{Ti} + ^{252}\text{Cf}$  combinations that have high probability to fuse together, forming the superheavy element with  $Z=120$ . So, the present study is carried out using 4 chosen reactions i.e.  $^{54}\text{Cr} + ^{248}\text{Cm}$ ,  $^{50}\text{Ti} + ^{252}\text{Cf}$  and  $^{50}\text{Ti} + ^{249}\text{Cf}$  and one with the traditional Ca-based hot fusion reaction  $^{48}\text{Ca} + ^{254}\text{Fm}$ , and effort has been made to predict their fusion cross-sections well below and above the Coulomb barrier, where the values for center of mass energies for reactions  $^{54}\text{Cr} + ^{248}\text{Cm}$  and  $^{50}\text{Ti} + ^{249}\text{Cf}$  are taken from reference [1]. Also, for the combination  $^{50}\text{Ti} + ^{252}\text{Cf}$ , we have taken the same energies values as for the combination  $^{50}\text{Ti} + ^{249}\text{Cf}$ , since they have nearly equal barrier heights (discussed later).

Firstly, the interaction potential  $V(\text{MeV})$  as a function of separation distance  $R(\text{fm})$  is calculated for four different entrance channels  $^{54}\text{Cr} + ^{248}\text{Cm}$ ,  $^{50}\text{Ti} + ^{252}\text{Cf}$ ,  $^{48}\text{Ca} + ^{254}\text{Fm}$  and  $^{50}\text{Ti} + ^{249}\text{Cf}$  and is shown in Fig.3.1, while taking the effect of quadrupole deformations and optimum orientations into account.

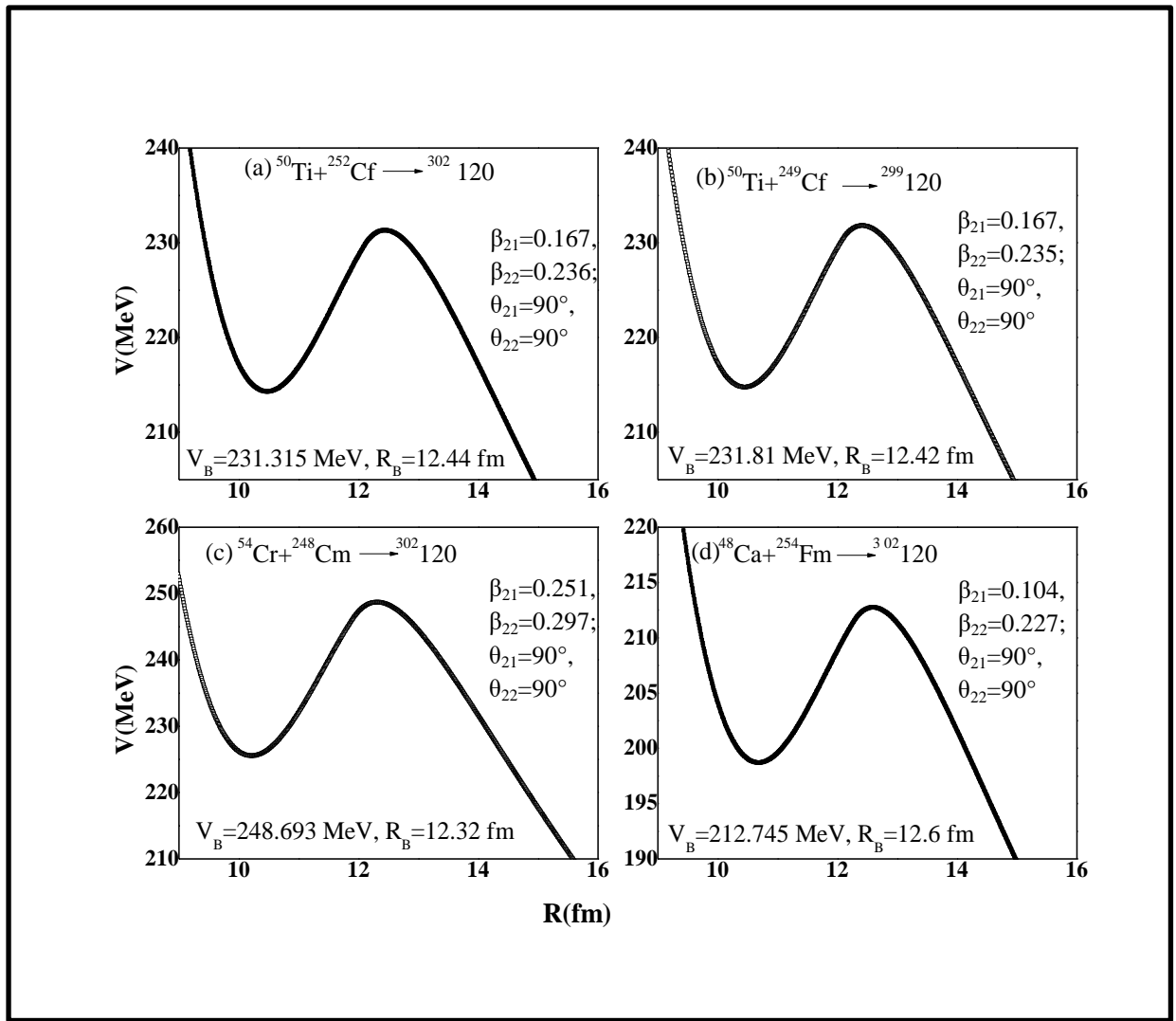


**Fig.3.1** Scattering potential vs separation distance  $R$  (fm) for four different entrance channels (a)  $^{50}\text{Ti} + ^{252}\text{Cf}$ , (b)  $^{50}\text{Ti} + ^{249}\text{Cf}$ , (c)  $^{54}\text{Cr} + ^{248}\text{Cm}$  and (d)  $^{48}\text{Ca} + ^{254}\text{Fm}$  at  $l=0$ ,  $T=0\text{MeV}$

Fig.3.1 shows the scattering potential of the four different target-projectile combinations i.e. (a)  $^{50}\text{Ti} + ^{252}\text{Cf}$ , (b)  $^{50}\text{Ti} + ^{249}\text{Cf}$ , (c)  $^{54}\text{Cr} + ^{248}\text{Cm}$  and (d)  $^{48}\text{Ca} + ^{254}\text{Fm}$ . It is clear from Fig.3.1 that for all the four chosen reactions, deep-well nuclear potential pocket is seen which seems suitable for heavy ion fusion reactions. As it is noticed that  $^{54}\text{Cr} + ^{248}\text{Cm}$  has the highest barrier at  $V_B = 248.693$  MeV due to the higher  $Z_1Z_2$  which increases the Coulomb repulsion between the collision partners. However, barrier height of Ti-projectile reactions i.e.  $^{50}\text{Ti} + ^{252}\text{Cf}$  and  $^{50}\text{Ti} + ^{249}\text{Cf}$  reactions which differ only in the number of neutrons possess almost similar barrier height i.e. 231.315 MeV and 231.81 MeV respectively. The fourth chosen reaction for  $Z=120$  i.e.  $^{48}\text{Ca} + ^{254}\text{Fm}$  has the lowest interaction barrier i.e.  $V_B = 212.745$  MeV among the four, due

to the low  $Z_1Z_2$  product, The values of  $Z_1Z_2$  product,  $\eta$  mass asymmetry,  $V_B$  barrier height,  $R_B$  barrier position and  $P_{CN}$  are tabulated for each reaction in Table 3.1.

**Table 3.1** Comparison of the fusion probabilities at the potential barrier, potential barrier for the hot- fusion combinations  $^{50}\text{Ti} + ^{252}\text{Cf}$ ,  $^{50}\text{Ti} + ^{249}\text{Cf}$ ,  $^{54}\text{Cr} + ^{248}\text{Cm}$  and  $^{48}\text{Ca} + ^{254}\text{Fm}$ .

Reaction	$Z_1Z_2$	$\eta = \frac{A_1 - A_2}{A_1 + A_2}$	$V_B$ (MeV)	$R_B$ (fm)	$P_{CN} (V_B)$
$^{54}\text{Cr} + ^{248}\text{Cm}$	2304	0.6423	248.694	12.32	2.0E-9
$^{50}\text{Ti} + ^{249}\text{Cf}$	2156	0.6655	231.811	12.42	3.2E-9
$^{50}\text{Ti} + ^{252}\text{Cf}$	2146	0.6688	231.315	12.44	4.7E-9
$^{48}\text{Ca} + ^{254}\text{Fm}$	2000	0.6821	212.6	12.6	5.5E-9

The above Table 3.1 gives a nice comparison about the barrier characteristics,  $Z_1Z_2$  product, mass symmetry, and the  $P_{CN}$  at the potential barrier among the all reactions, which gives the nice details about the nuclear fusion reaction dynamics for the following reactions. It is observed that with the increase in the charge symmetry, the barrier height increases and the interaction radius decreases.

After the calculations of scattering potential, the capture cross-sections are calculated at energies around these maximum values of potential barrier (taking round-off values). As mentioned earlier in Chapter 2, in the case of superheavy nuclei, the capture cross-section cannot alone predict about the formation of compound nucleus. Thus, we have tried to find the fusion cross-section as the product of capture cross-section and probability of compound nucleus formation  $P_{CN}$  that gives the possibility of the compound nucleus formation using  $\beta_2$ -deformed fragments. Using Wong formula and eq. (2.7) for  $P_{CN}$ , the cross-sections are calculated for the four different chosen reactions. The calculated values of capture cross-sections, probability of compound nucleus  $P_{CN}$  and hence fusion cross-sections for the four different systems are given under in Table 3.2 3.3, 3.4 and 3.5 for  $^{54}\text{Cr} + ^{248}\text{Cm}$ ,  $^{50}\text{Ti} + ^{249}\text{Cf}$ ,  $^{50}\text{Ti} + ^{252}\text{Cf}$  and  $^{48}\text{Ca} + ^{254}\text{Fm}$  respectively.

**Table 3.2** The calculated values of fusion cross-sections and  $P_{CN}$  for  $^{54}\text{Cr} + ^{248}\text{Cm}$ .

$E_{CM}$	$\sigma_{capture}$ (mb)	$P_{CN}$	$\sigma_{fus} = \sigma_{capture} * P_{CN}$
237.2	143.0114	2.34E-10	334.6466E-10
241.5	222.8898	6E-10	1337.3388E-10
246.7	334.4342	1.5E-9	501.6513E-9
248.2	368.2678	2E-9	736.8684E-9
249.6	399.8557	2.3E-9	919.6681E-9
252.0	453.3100	2.31E-9	104.71461E-8

The above Table 3.2 depicts the predicted values of capture cross-section,  $P_{CN}$  and fusion cross-sections for the  $^{54}\text{Cr} + ^{248}\text{Cm}$  reaction calculated at center of mass energies (MeV) 237.2, 241.5, 246.7, 248.2, 249.6 and 252.0 taken from reference [1], well below and above the potential barrier which was at 248.694 MeV. It is observed that with the increase in energy, fusion cross-section increases and deformations along with optimum orientations affect the fusion cross-sections as they significantly affect the barrier characteristics.

**Table 3.3** The calculated values of fusion cross-sections and  $P_{CN}$  for  $^{50}\text{Ti} + ^{249}\text{Cf}$ .

$E_{CM}$	$\sigma_{capture}$ (mb)	$P_{CN}$	$\sigma_{fus} = \sigma_{capture} * P_{CN}$
225	132.1124	1.03E-9	136.0757E-9
227	171.9770	1.544E-9	265.5324E-9
231.5	275.3052	3.2E-9	880.9766E-9
236	380.7958	4.8E-9	182.78198E-8
237.2	408.3046	5.1E-9	208.23584E-8
241.5	505.1037	5.8E-9	292.96014E-8

**Table 3.4** The calculated values of fusion cross-sections and  $P_{CN}$  for  $^{50}\text{Ti} + ^{252}\text{Cf}$ .

$E_{CM}$	$\sigma_{capture}$ (mb)	$P_{CN}$	$\sigma_{fus} = \sigma_{capture} * P_{CN}$
225	145.1521	1.697E-9	246.3231E-9
227	186.5538	1.7E-9	317.1E-9
231.3	287.3351	4.7E-9	135.04E-8

236	398.1676	7.28E-9	289.8E-8
237.2	425.8234	7.7E-9	327.88E-8
241.5	522.748	8.8E-9	460.01E-8

**Table 3.5** The calculated values of fusion cross-sections and  $P_{CN}$  for  $^{48}\text{Ca} + ^{254}\text{Fm}$ .

$E_{CM}$	$\sigma_{capture}$ (mb)	$P_{CN}$	$\sigma_{fus} = \sigma_{capture} * P_{CN}$
208	120.1681	2.6E-9	312.4370E-9
210	162.5898	3.7E-9	601.5822E-9
212.6	226.5183	5.5E-9	124.58506E-8
214	262.8134	6.4E-9	168.20057E-8
216	314.1152	7.6E-9	238.72755E-8

Similarly, the Table 3.3, 3.4 and 3.5 same as Table 3.2 but for the different reactions i.e.  $^{50}\text{Ti} + ^{249}\text{Cf}$ ,  $^{50}\text{Ti} + ^{252}\text{Cf}$  and  $^{48}\text{Ca} + ^{254}\text{Fm}$  respectively depict the capture cross-sections,  $P_{CN}$  and fusion cross-sections calculated in the same manner. For the reactions  $^{50}\text{Ti} + ^{249}\text{Cf}$  and  $^{50}\text{Ti} + ^{252}\text{Cf}$ , the center of mass energies are taken corresponding to their barrier potentials from reference [1] and for the combination  $^{48}\text{Ca} + ^{254}\text{Fm}$  the center of mass energies are taken  $\pm 4$  MeV across the Coulomb barrier. It is clearly noticed that the maximum fusion cross-section for  $^{54}\text{Cr} + ^{248}\text{Cm}$ ,  $^{50}\text{Ti} + ^{252}\text{Cf}$ ,  $^{50}\text{Ti} + ^{249}\text{Cf}$  and  $^{48}\text{Ca} + ^{254}\text{Fm}$  are 1047.1461pb, 4600.1pb, 2929.601pb and 2387.2pb at energies 252 MeV, 241.5 MeV, 241.5 MeV and 216 MeV respectively at highest energies relative to their corresponding barrier heights. Since the energies range for the chosen reaction is different across the barrier, so the comparison is made at the Coulomb barrier and then 4 MeV above the Coulomb barrier. The reactions  $^{50}\text{Ti} + ^{252}\text{Cf}$  and  $^{48}\text{Ca} + ^{254}\text{Fm}$  give the maximum fusion cross-sections at their corresponding barrier heights. However, the fusion cross-sections of each reaction at 4 MeV above the Coulomb barrier notifies that  $^{50}\text{Ti}$  beam provides better results. Although, with the  $^{48}\text{Ca}$ -projectile reaction, we have the lowest barrier and also provides better fusion cross-sections at much lower energies than the others, but  $^{254}\text{Fm}$  being not so efficiently available target till to-date. Thus, we conclude that the instead of  $^{48}\text{Ca}$ -beam projectile  $^{50}\text{Ti}$ -beam could serve our purpose more effectively, since the  $^{54}\text{Cr} + ^{248}\text{Cm}$  entrance system also provides the highest fusion hindrance and being heavier projectile requires more energy than the Ca and Ti projectile.

Therefore, in future we could use  $^{48}\text{Ca} + ^{254}\text{Fm}$  reaction to synthesize the  $Z=120$ , if we are able to make  $^{254}\text{Fm}$  as a perfect target. However for now, besides the tradition i.e.  $^{48}\text{Ca}$ -based hot fusion reactions, one could move towards the reactions  $^{50}\text{Ti} + ^{252}\text{Cf}$  and  $^{50}\text{Ti} + ^{249}\text{Cf}$  providing the compound nucleus  $^{302}120$  and  $^{299}120$  respectively for future experiments in the search of next magic shell closure.

### 3.2 The study of cold valley regions of $^{302}120$ using Fragmentation Potential

Besides the four chosen reactions, an attempt is made to analyze the different projectile-target combinations, which are taken from “cold valley” of fragmentation potential.

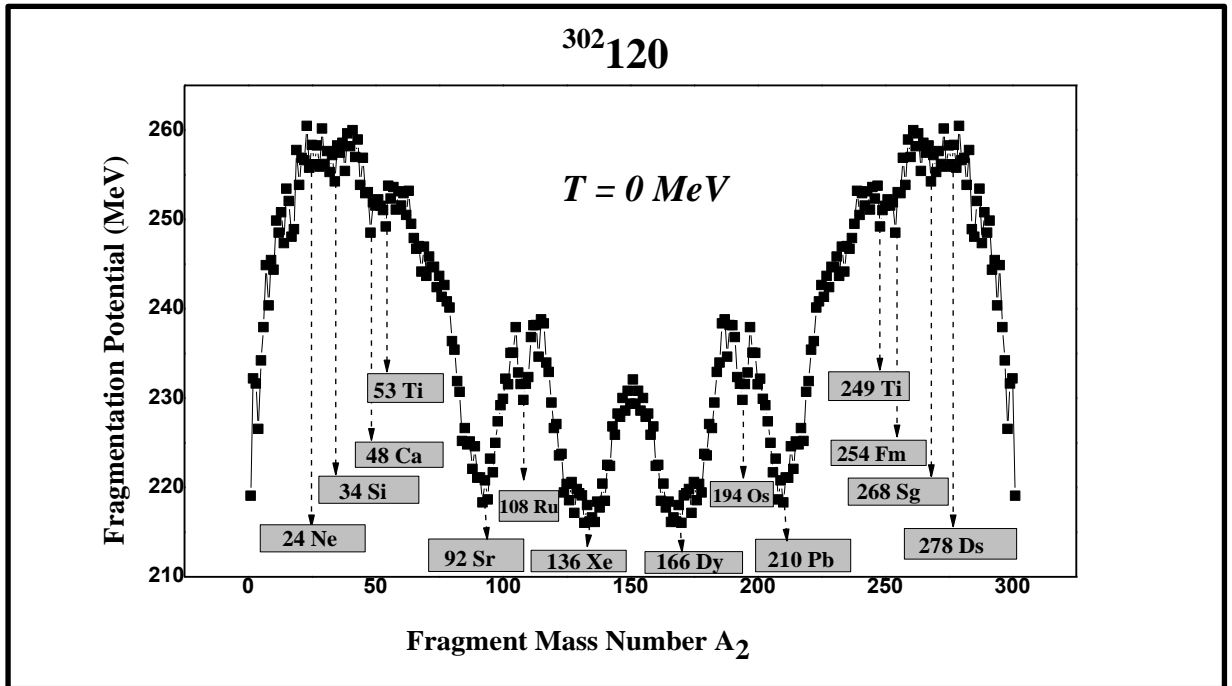


**Fig.3.2** Fragmentation potential v/s mass fragment  $A_2$  at  $\ell=0\hbar$ ,  $T=0$  MeV and  $\Delta R=1.5$  fm

The fragmentation potential is plotted as a function of mass fragment  $A_2$  at  $T=0$  MeV with  $\Delta R=1.5$  fm. The neck of 1.5 fm is taken fixed for  $^{302}120$  nuclei, since the nucleus is large in size so neck-length is taken large as well. “The cold valleys” of Fig.3.2 provides the probable target-projectile combinations i.e.  $^{24}\text{Ne} + ^{278}\text{Ds}$ ,  $^{34}\text{Si} + ^{268}\text{Sg}$ ,  $^{48}\text{Ca} + ^{254}\text{Fm}$ ,  $^{53}\text{Ti} + ^{249}\text{Cf}$ ,  $^{92}\text{Sr} +$

$^{210}\text{Pb}$ ,  $^{108}\text{Ru} + ^{194}\text{Os}$ ,  $^{136}\text{Xe} + ^{166}\text{Dy}$ . Here,  $^{48}\text{Ca} + ^{254}\text{Fm}$  appearing in cold-valley region, confirms our choice of taking this combination in previous section 3.1. Also, it was inferred from Section 3.1 that  $^{48}\text{Ca} + ^{254}\text{Fm}$  provides better fusion cross-section, therefore could be probably better target-projectile combination if  $^{254}\text{Fm}$  becomes available to us as a target.

To investigate the effect of temperature on most probable target-projectile combinations, the fragmentation potential is plotted as a function of mass fragment  $A_2$  at  $\ell = 0\hbar$  and  $\ell = \ell_{\max}$  as shown in Fig.3.3 and 3.4 respectively at  $T=1$  MeV.

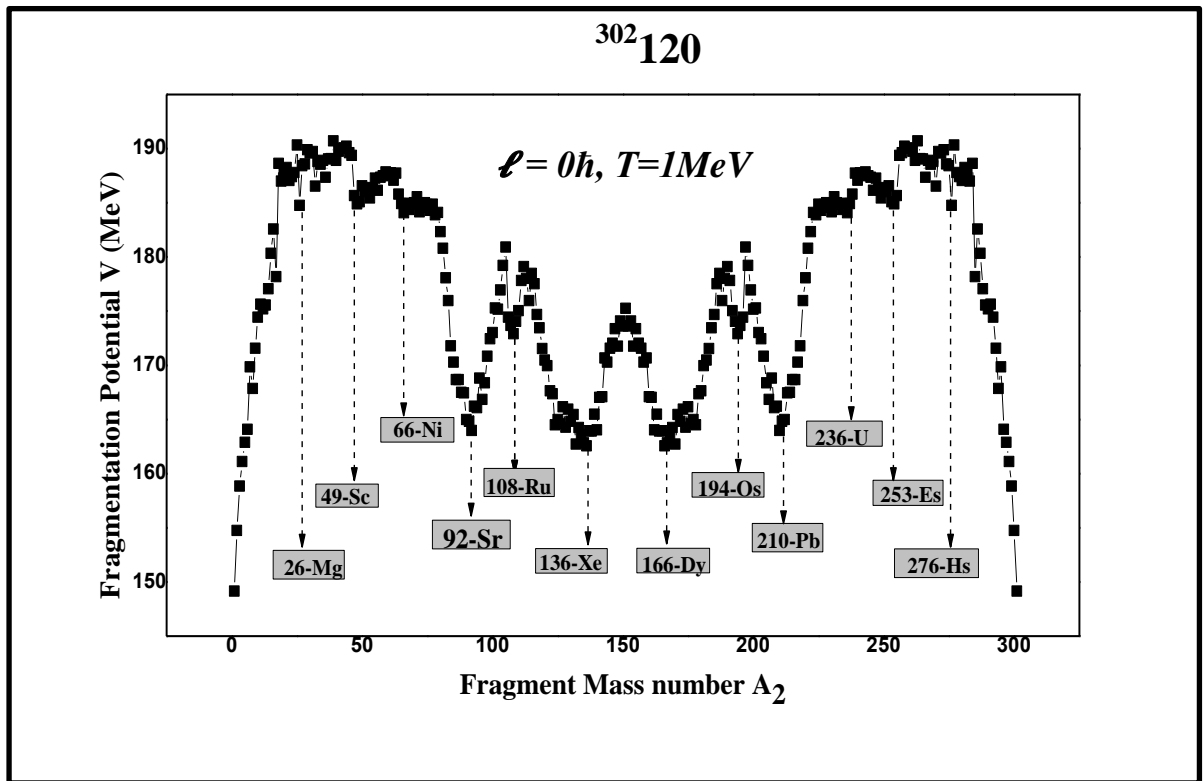


**Fig.3.3** Fragmentation potential v/s mass fragment  $A_2$  at  $\ell = 0\hbar$ ,  $T=1$  MeV and  $\Delta R = 1.5$  fm for the decay of  $^{302}_{120}$  nuclei

In Fig.3.3, shows the fragmentation potential for the compound nucleus  $^{302}_{120}$  at  $\ell = 0\hbar$ , at  $T=1.0$  MeV, with  $\Delta R = 1.5$  fm. From the plot, observing the deep cold regions, some more probable combinations are noticed at  $^{26}\text{Mg} + ^{276}\text{Hs}$ ,  $^{49}\text{Sc} + ^{253}\text{Es}$ ,  $^{66}\text{Ni} + ^{236}\text{U}$ ,  $^{92}\text{Sr} + ^{210}\text{Pb}$ ,  $^{108}\text{Ru} + ^{194}\text{Os}$ ,  $^{136}\text{Xe} + ^{166}\text{Dy}$ .

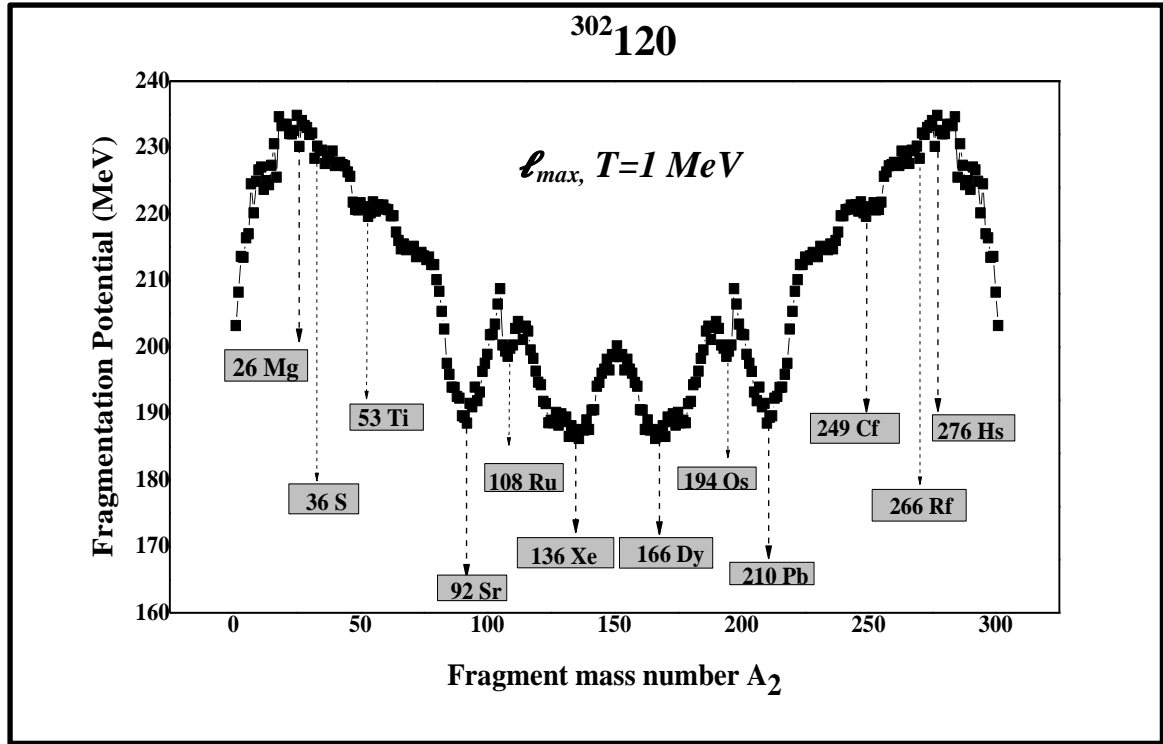


**Fig.3.4** Fragmentation potential v/s mass fragment  $A_2$  at  $\ell = \ell_{max}$ ,  $T=1$  MeV and  $\Delta R = 1.5$  fm for the decay of  $^{302}120$  nuclei

Similarly, the fragmentation potential is plotted for  $^{302}120$  at  $\ell = \ell_{max} = 140\hbar$ , with same temperature and  $\Delta R$  as for Fig.3.3. Note that, here  $\ell = \ell_{max}$  is decide at a point when penetrability,  $P_\ell = 1$ . The behavior of both plots is almost the same and here the deep minima's giving combinations are  $^{26}\text{Mg} + ^{276}\text{Hs}$ ,  $^{36}\text{S} + ^{266}\text{Rf}$ ,  $^{53}\text{Ti} + ^{249}\text{Cf}$ ,  $^{92}\text{Sr} + ^{210}\text{Pb}$ ,  $^{108}\text{Ru} + ^{194}\text{Os}$ ,  $^{136}\text{Xe} + ^{166}\text{Dy}$ .

The interaction potential  $V$  (MeV) for the obtained combinations with well-deep minima's in the Fig.3.3 and 3.4, is plotted against the separation distance  $R$  (fm) shown in Fig.3.5, on considering the  $\beta_2$  deformations and "hot-compact" optimum orientations with zero angular momentum values  $\ell=0$  and  $T=0$  MeV, in the question of finding the most suitable combination reaction.

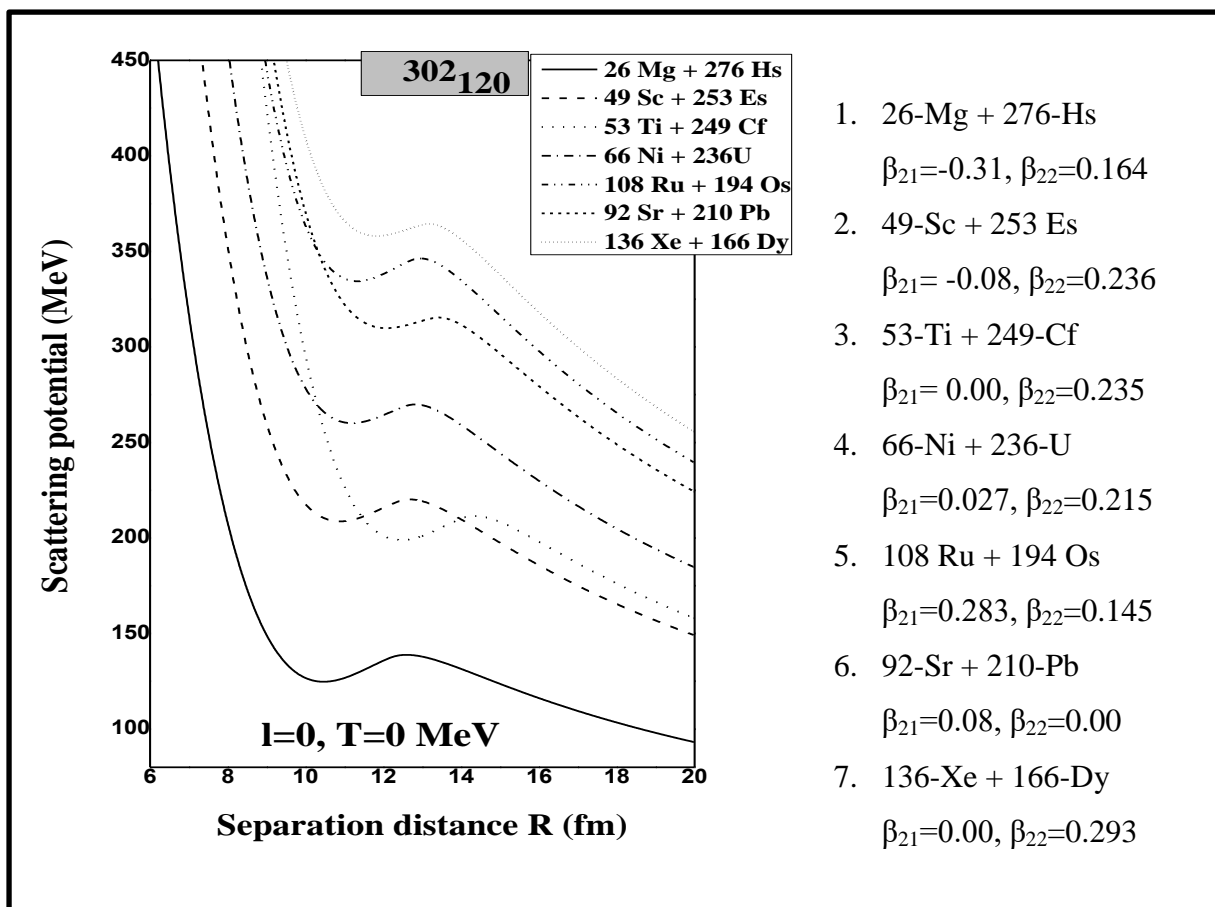


**Fig.3.5** Scattering potential vs separation distance  $R$  (fm) for the obtained reactions from minima's in fragmentation plot. (See Fig. 3.3 and 3.4)

From the plot, it was found the maximum barrier potential for the combinations  $^{26}\text{Mg} + ^{276}\text{Hs}$ ,  $^{49}\text{Sc} + ^{253}\text{Es}$ ,  $^{53}\text{Ti} + ^{249}\text{Cf}$ ,  $^{66}\text{Ni} + ^{236}\text{U}$ ,  $^{92}\text{Sr} + ^{210}\text{Pb}$ ,  $^{108}\text{Ru} + ^{194}\text{Os}$ ,  $^{136}\text{Xe} + ^{166}\text{Dy}$  comes out to be at 142.076 MeV, 223.215 MeV, 211.551 MeV, 269.904 MeV, 315.42 MeV, 346.326 MeV, 361.885 MeV, 364.422 MeV respectively and it can be inferred that the barrier height for the combination  $^{26}\text{Mg} + ^{276}\text{Hs}$  is found to be very low. However,  $^{276}\text{Hs}$  having very short lifetime of 1.11hr, so could not be able to serve our purpose. The second and third lowest barrier is 211.551 MeV and 223.215 MeV for  $^{53}\text{Ti} + ^{249}\text{Cf}$  and  $^{49}\text{Sc} + ^{253}\text{Es}$  respectively, however these two nuclei are odd-odd combination and hence it becomes difficult to synthesize  $Z=120$  nuclei with these combinations. Hence, the next probable combination comes out to be at  $^{66}\text{Ni} + ^{236}\text{U}$ .

## SUMMARY and CONCLUSIONS

1. The hot fusion reactions in the synthesis of superheavy nuclei using Ca-projectile beams is not reachable at reasonable rates for  $Z > 118$ , since they don't provide enough number of protons. Thus, we way toward the fusion of Ti- and Cr-beams with the transuranium elements to predict the superheavy ones with the greater number of protons than the existing ones. The new nuclei, obviously the stable ones would be important for studies of the nuclear physics and the chemistry of transactinide elements and also in the search of next Stable Island after 114.

2. In the present work, we have predicted the fusion cross-sections for the four hot fusion reactions  $^{54}\text{Cr} + ^{248}\text{Cm}$ ,  $^{50}\text{Ti} + ^{252}\text{Cf}$ ,  $^{50}\text{Ti} + ^{249}\text{Cf}$  and  $^{48}\text{Ca} + ^{254}\text{Fm}$  forming  $Z = 120$  element, where the analysis is done with the framework of Wong formula. The fusion cross-sections are investigated at the center of mass energies well above and below the Coulomb barrier, after analyzing the interaction plot, which gave higher barrier for  $^{54}\text{Cr} + ^{248}\text{Cm}$  at 248.693 MeV and lowest for  $^{48}\text{Ca} + ^{254}\text{Fm}$  at 212.745 MeV. However, the barrier potential obtained for  $^{50}\text{Ti} + ^{252}\text{Cf}$  and  $^{50}\text{Ti} + ^{249}\text{Cf}$  reactions are almost same i.e. 231.315 MeV and 231.81 MeV respectively. The fusion cross-section are calculated alongwith the calculations of  $P_{\text{CN}}$  as shown in Table 3.2, 3.3, 3.4 and 3.5 for all the four channels. It can be clearly noticed that the maximum fusion cross-section for  $^{54}\text{Cr} + ^{248}\text{Cm}$ ,  $^{50}\text{Ti} + ^{249}\text{Cf}$ ,  $^{50}\text{Ti} + ^{252}\text{Cf}$  and  $^{48}\text{Ca} + ^{254}\text{Fm}$  are 1047.1461 pb, 4600.1pb, 2929.601pb and 2387.2pb at energies 252 MeV, 241.5 MeV, 241.5 MeV and 216 MeV respectively, that are taken relative to their corresponding interaction potential barriers. However, when comparison is made at the respective Coulomb barriers of the four chosen reactions, the combinations  $^{50}\text{Ti} + ^{252}\text{Cf}$  and  $^{48}\text{Ca} + ^{254}\text{Fm}$  give maximum cross-sections. After, that we compare the results at the energies 4 MeV (for the sake of comparison) above their corresponding Coulomb barriers, it is found that the both Ti-beam reactions provide greater cross-sections. Thus, the results show that the  $^{50}\text{Ti}$  and  $^{249,152}\text{Cf}$  should be the most favorable projectile-target combinations for synthesis of new superheavy element  $Z=120$  theoretically. The whole set of calculations are done while taking the effects of  $\beta_2$ -deformations and optimum orientations along the collision axis for the most compact "hot configurations".

3. After the study of formation process of  $Z=120$  via different hot-fusion reactions, cold valley regions of  $^{302}120$  are studied using the fragmentation potential. From the fragmentation

at T=0 MeV, the combinations appear are  $^{24}\text{Ne} + ^{278}\text{Ds}$ ,  $^{34}\text{Si} + ^{268}\text{Sg}$ ,  $^{48}\text{Ca} + ^{254}\text{Fm}$ ,  $^{53}\text{Ti} + ^{249}\text{Cf}$ ,  $^{92}\text{Sr} + ^{210}\text{Pb}$ ,  $^{108}\text{Ru} + ^{194}\text{Os}$ ,  $^{136}\text{Xe} + ^{166}\text{Dy}$ , hence confirm our choice of taking  $^{48}\text{Ca} + ^{254}\text{Fm}$  as target-projectile combination in section 3.1. From the fragmentation plot Fig.3.3 and 3.4, using the concept that deep minima in these plot that corresponds to the most probable projectile-target combinations for fusion are  $^{26}\text{Mg} + ^{276}\text{Hs}$ ,  $^{49}\text{Sc} + ^{253}\text{Es}$ ,  $^{53}\text{Ti} + ^{249}\text{Cf}$ ,  $^{66}\text{Ni} + ^{236}\text{U}$ ,  $^{92}\text{Sr} + ^{210}\text{Pb}$ ,  $^{108}\text{Ru} + ^{194}\text{Os}$ ,  $^{136}\text{Xe} + ^{166}\text{Dy}$ , plotted at  $\ell=0\hbar$  and  $\ell_{\text{max}}=140\hbar$  respectively at T=1 MeV. We have calculated the potential barriers for the combinations obtained from Fig.3.3 and 3.4, while considering the  $\beta_2$  deformations and hot optimum orientations with zero angular momentum values  $\ell=0$  and T=0 MeV and was found to be minimum for  $^{26}\text{Mg} + ^{276}\text{Hs}$  i.e. at 142.076MeV can't be used since  $^{276}\text{Hs}$  has very short life-time while the next combinations with lower barrier are  $^{53}\text{Ti} + ^{249}\text{Cf}$ ,  $^{49}\text{Sc} + ^{253}\text{Es}$ , being odd-odd nuclei so it is not easy to use these target-projectile combinations. Also the combinations,  $^{92}\text{Sr} + ^{210}\text{Pb}$ ,  $^{108}\text{Ru} + ^{194}\text{Os}$ ,  $^{136}\text{Xe} + ^{166}\text{Dy}$  are having greater charge symmetry, hence making it difficult for fusion to happen in competition to fission. Therefore,  $^{66}\text{Ni} + ^{236}\text{U}$  could be able serve our purpose if both 66-Ni and U-236 are available as projectile and target respectively experimentally.

Finally through our study, it was predicted that the  $^{50}\text{Ti} + ^{252}\text{Cf}$  and  $^{50}\text{Ti} + ^{249}\text{Cf}$  has the maximum cross-section for Z=120 among the four chosen  $^{54}\text{Cr} + ^{248}\text{Cm}$ ,  $^{50}\text{Ti} + ^{252}\text{Cf}$ ,  $^{50}\text{Ti} + ^{249}\text{Cf}$  and  $^{48}\text{Ca} + ^{254}\text{Fm}$  forming Z= 120 element and the new combination  $^{26}\text{Mg} + ^{276}\text{Hs}$ ,  $^{49}\text{Sc} + ^{253}\text{Es}$ ,  $^{53}\text{Ti} + ^{249}\text{Cf}$ ,  $^{66}\text{Ni} + ^{236}\text{U}$ ,  $^{92}\text{Sr} + ^{210}\text{Pb}$ ,  $^{108}\text{Ru} + ^{194}\text{Os}$ ,  $^{136}\text{Xe} + ^{166}\text{Dy}$  were found for the formation of compound nucleus with Z=120.

## REFERENCES

- [1] A. K. Nasirov, G. Mandaglio, G. Giardina, A. Sobiczewski, and A. I. Muminov, Phys. Rev. C 84, 044612 (2011).
- [2] Z. H. Liu and J. D. Bao, Phys. Rev. C 80, 054608 (2009).
- [3] V. Zagrebaev and W. Greiner, Phys. Rev. C 78, 034610 (2008).